

Effect of magnetic field on positron lifetimes of Fe, Co and Ni

This content has been downloaded from IOPscience. Please scroll down to see the full text.

2015 J. Phys.: Condens. Matter 27 246001

(<http://iopscience.iop.org/0953-8984/27/24/246001>)

View [the table of contents for this issue](#), or go to the [journal homepage](#) for more

Download details:

IP Address: 133.53.196.196

This content was downloaded on 07/07/2015 at 00:22

Please note that [terms and conditions apply](#).

Effect of magnetic field on positron lifetimes of Fe, Co and Ni

H Li¹, M Maekawa¹, A Kawasuso¹ and N Tanimura²

¹ Advanced Science Research Center, Japan Atomic Energy Agency, 1233 Watanuki, Takasaki, Gunma JP-370-1292, Japan

² Science Solution Division, Mizuho Information and Research Institute, 2-3, Kanda-Nishikicho, Chiyoda-ku, Tokyo, 101-8443, Japan

E-mail: li.hui@jaea.go.jp

Received 26 December 2014, revised 9 April 2015

Accepted for publication 20 April 2015

Published 3 June 2015



Abstract

Positron lifetime spectra of Fe, Co and Ni were measured under magnetic field using a ²²Na source. Very small but distinguishable difference of positron lifetime upon magnetic field reversal was observed suggesting the existence of two bulk lifetimes associated with majority and minority spin electrons. Using two spin-dependent Fe bulk lifetimes, the difference Doppler broadening of annihilation radiation spectra between majority and minority spin electrons were also examined. Agreement between experiment and theory indicates that spin-polarized positron annihilation spectroscopy may have potential in investigation of spin-aligned electron momentum distribution.

Keywords: spin-polarized positron lifetime, Fe, Co and Ni, Doppler broadening of annihilation radiation

(Some figures may appear in colour only in the online journal)

1. Introduction

After the discovery of parity non-conservation in the weak interaction [1, 2], spin-polarized positrons from radioisotopes were used in the angular correlation of annihilation radiation (ACAR) experiments for studying ferromagnetic band structures [3–20]. The half-metallicity of NiMnSb was shown for the first time by using spin-polarized two-dimensional ACAR [20, 21]. Some reports also show that even non-polarized positrons are useful to probe Fermi surfaces of ferromagnets [22, 23]. Recently, we demonstrated that the Doppler broadening of annihilation radiation (DBAR) technique using ²²Na and ⁶⁸Ge–⁶⁸Ga sources are also useful for similar purposes [24–27]. These methods are analogous to the magnetic Compton profiling (MCP) [28, 29]. However, as compared to MCP, in ACAR and DBAR cases, to obtain direct difference spectra between majority and minority spin bands, the spectrum measured in magnetic field needs to be renormalized using the total annihilation rate of spin-up and spin-down positrons or by field-reversal of three-gamma annihilation probability. Berko and Mills attempted to measure the latter [6]. However, its precise determination was not

easy because of the extremely low three-fold coincidence rate (~ 1 cps). To determine the total annihilation rates of spin-up and spin-down positrons, spin-polarized positron lifetime measurement, which has not yet been carried out except for previously considering asymmetry of counts in the selected region from the lifetime spectrum [30, 31], is important. Recently, a theoretical work implied the observable differences of positron lifetimes associated with majority and minority spin electrons in Fe, Co and Ni [32].

In this study, we measured the spin-dependent positron lifetimes in Fe, Co and Ni. Using the spin-dependent lifetimes in Fe, we also examined the direct difference DBAR spectra associated with majority and minority spin electrons.

2. Theory

The total annihilation rate of spin-up (spin-down) positrons is given by [6]

$$\lambda^{\uparrow(\downarrow)} = \frac{1}{2} \sum_{i=1}^{\text{occ}} [\lambda_S w_i^{\downarrow(\uparrow)} + \lambda_T (w_i^{\downarrow(\uparrow)} + 2w_i^{\uparrow(\downarrow)})], \quad (1)$$

where the majority spin band is described as \downarrow (magnetic momentum is up) and minority spin band is expressed as \uparrow (magnetic momentum is down); $\lambda_S = 4\pi r_e^2 c$, where r_e is the classical electron radius and c is light speed; $\lambda_T = \lambda_S/1115$, where 1115 is the ratio of the decay constants between singlet and triplet positron-electron pairs [33], and $w_i^{\downarrow(\uparrow)}$ is the overlap integral between the positron and the i -th majority(minority) spin-band wave functions, which is given by [6, 25]

$$w_i^{\downarrow(\uparrow)} = \int n_i^{\downarrow(\uparrow)}(\mathbf{r})n_+(\mathbf{r})\gamma[n_-(\mathbf{r})]d\mathbf{r}, \quad (2)$$

where $n_i^{\downarrow(\uparrow)}(\mathbf{r})$ is the electron density of the i -th majority(minority) spin-band, $n_+(\mathbf{r})$ is the positron density and $\gamma[n_-(\mathbf{r})]$ is the enhancement factor [34]. In positive and negative magnetic fields, positron lifetime spectrum is given by

$$L_{\pm}(t) = \frac{\lambda_S}{4} \sum_i^{\text{occ}} [w_i^{\downarrow}(1 \pm P)e^{-\lambda_{\uparrow}^{\downarrow}t} + w_i^{\uparrow}(1 \mp P)e^{-\lambda_{\uparrow}^{\uparrow}t}], \quad (3)$$

where P is the positron spin polarization. The field direction is defined as positive (negative) when its orientation is the same as (opposite to) that of positron spin polarization. Due to the difference of electron densities between majority and minority spin bands in ferromagnets, corresponding two bulk lifetimes exist.

The first and second terms in the brace of equation (1) correspond to two-gamma and three-gamma events, respectively. Therefore, $\lambda_{\uparrow}^{\downarrow(\uparrow)} = \lambda_{\text{maj}(\text{min})} + (\lambda_{\text{maj}(\text{min})} + 2\lambda_{\text{min}(\text{maj})})/1115$, where $\lambda_{\text{maj}(\text{min})} (= \tau_{\text{maj}(\text{min})}^{-1})$ denotes the two-gamma annihilation rate (inverse of lifetime) of positrons with majority (minority) spin electrons. Two-gamma positron annihilation rate in positive(negative) magnetic field is given by

$$\lambda_{\pm}(= \tau_{\pm}^{-1}) = \frac{1 \pm P}{2} \lambda_{\text{maj}} + \frac{1 \mp P}{2} \lambda_{\text{min}}. \quad (4)$$

The DBAR spectrum in magnetic field is given by [6, 25]

$$N_{\pm}(p_z) = \frac{\lambda_S}{4} \sum_{i=1}^{\text{occ}} \left[\frac{(1 \pm P)N_i^{\downarrow}(p_z)}{\lambda_{\uparrow}^{\downarrow}} + \frac{(1 \mp P)N_i^{\uparrow}(p_z)}{\lambda_{\uparrow}^{\uparrow}} \right], \quad (5)$$

where $N_i^{\downarrow(\uparrow)}(p_z)$ is the DBAR spectrum :

$$N_i^{\downarrow(\uparrow)}(p_z) = \int \int \rho_i^{\downarrow(\uparrow)}(\mathbf{p})dp_x dp_y. \quad (6)$$

Here, $\rho_i^{\downarrow(\uparrow)}(\mathbf{p})$ are the positron-electron-momentum densities for the i th majority (and minority) spin bands given by [25]

$$\rho_i^{\downarrow(\uparrow)}(\mathbf{p}) = \left| \int e^{-i\mathbf{p}\cdot\mathbf{r}} \Psi_+(\mathbf{r})\Psi_i^{\downarrow(\uparrow)}(\mathbf{r})\sqrt{\gamma[n_-(\mathbf{r})]}d\mathbf{r} \right|^2, \quad (7)$$

where $\Psi_+(\mathbf{r})$ is the positron wave function, $\Psi_i^{\downarrow(\uparrow)}(\mathbf{r})$ is the electron wave function.

The difference DBAR spectrum between majority and minority spin bands is given by [25]

$$\sum_{i=1}^{\text{occ}} [N_i^{\downarrow}(p_z) - N_i^{\uparrow}(p_z)] \propto \Delta N(p_z) - P_{\lambda} \Sigma N(p_z), \quad (8)$$

where $\Delta N(p_z) = N_+(p_z) - N_-(p_z)$, $\Sigma N(p_z) = N_+(p_z) + N_-(p_z)$, $P_{\lambda} = P(\lambda^{\downarrow} - \lambda^{\uparrow})/(\lambda^{\downarrow} + \lambda^{\uparrow})$ and $\int N_{\pm}(p_z)dp_z$ is normalized to unity. Berko and Mills [6] suggested that the field-reversal of three-gamma annihilation probability, $P^{3\gamma} = (N_+^{3\gamma} - N_-^{3\gamma})/(N_+^{3\gamma} + N_-^{3\gamma})$, is approximately equal to P_{λ} .

In this work, the difference DBAR spectra for individual bands of Fe were theoretically calculated. The electron wave functions were obtained from the ABINIT computation [35] with the projector-augmented-wave method [36]. The initial valence electron configurations were assumed to be $3d^6 4s^2$. The positron wave function was calculated based on the two-component density functional theory. The DBAR spectrum was obtained by double-integrating the momentum density with a Gaussian convolution having the full width at half maximum of 1.4 keV. The details of the calculation were described elsewhere [25].

3. Experiment

The samples used in this work were polycrystalline Fe(4N), Co(5N), Ni(5N) and Cu(4N), and single crystal Fe(1 0 0) and Fe(1 1 1) discs with 10 mm diameter and 1 or 2 mm thickness. All the samples were electrochemically polished on one side. The Fe, Co and Ni samples were annealed at 1200 °C for 2 h in vacuum. The Cu samples were annealed at 1000 °C for 3 h in vacuum.

A ^{22}Na positron source of 1 MBq was deposited onto a Ti film (5 μm thick). The source was sandwiched by an Fe, Co, Ni or Cu sample with a Cu sample and the sample-source pairs were horizontally placed in the gap of two permanent magnets arranged vertically where the magnetic field was ± 1 T. If both sides of the source are ferromagnetic samples, no field reversal asymmetry of positron lifetime should be observed due to opposite positron spin polarizations for opposite directions. Positron lifetime spectra were measured using a fast-fast coincidence system and two Hamamatsu H3378-50 photomultipliers coupled with plastic scintillators of sizes of 30 mm in height and 20 mm in diameter. One spectrum contained more than 1×10^6 counts. After finishing each lifetime measurement, the sample-source face was reversed with respect to the field direction. No serious influence of the fringing field to the lifetime measurement system was confirmed from the measurements without magnetic field. Longitudinal spin polarization of positrons was $P = 35\%$ [37].

The obtained lifetime spectra were decomposed into three lifetime components by the PATFIT program [38]. The first component (τ_1, I_1 , where τ and I denote lifetime and intensity, respectively) was attributed to positron annihilation in the bulk. The second ($\tau_2 \sim 269$ ps, $I_2 \sim 26\%$) and third ($\tau_3 \sim 1.4$ ns, $I_3 \sim 2.2\%$) components were due to annihilation of positrons in the source and the space between the samples and the source, respectively. The intensity of source annihilation in thick Ti foil covering ^{22}Na was significant, however, these two lifetimes were longer than the first lifetime and easily separated from lifetime spectra. The half of positrons were assumed to annihilate in one of the sandwiching samples and hence the bulk lifetimes of ferromagnet samples in positive (negative)

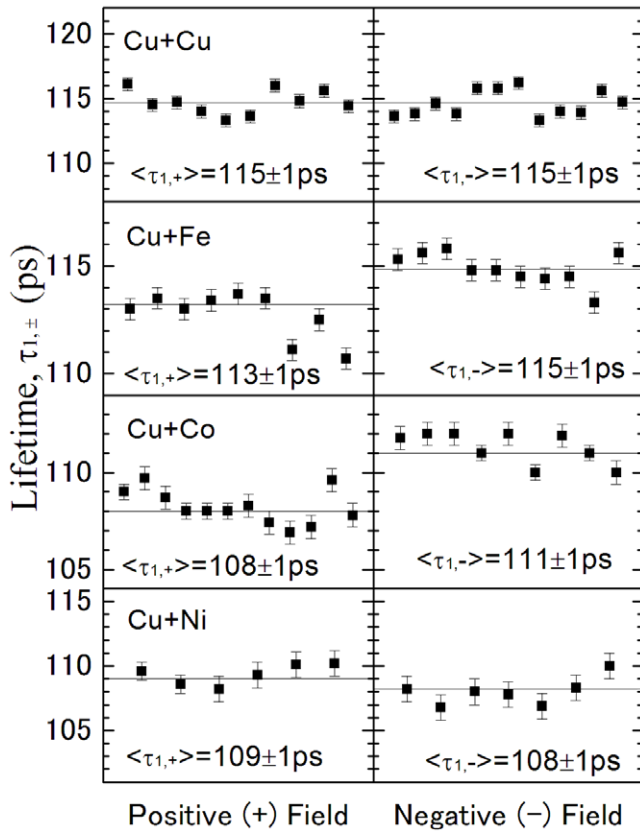


Figure 1. The first lifetimes ($\tau_{1,\pm}$) for the Cu + Cu, Fe + Cu, Co + Cu and Ni + Cu samples under magnetic field of ± 1 T.

magnetic field were deduced by

$$\tau_{\pm} = 2\tau_{1,\pm} - \tau_{Cu}. \quad (9)$$

The uncertainty due to subtraction of 50% Cu was low. We calculated the transportation of error and obtained typical final error bar to be less than 1 ps. DBAR spectra were measured by using a high-purity Ge detector with an energy resolution of 1.4 keV at 511 keV as described elsewhere [25]. The source was a 20 MBq ^{68}Ge - ^{68}Ga and the average spin polarization was 60%. Here, gamma-ray energy of 1 keV corresponds to an electron momentum of $p = 3.92 \times 10^{-3} m_0c$ (0.54 a.u.). In each spectrum, more than 10^6 events were accumulated.

4. Results and discussion

The bulk lifetimes obtained without magnetic field were 114 ± 1 ps (Cu), 109 ± 1 ps (Fe), 109 ± 1 ps (Co), and 101 ± 1 ps (Ni). These are in good agreement with previous experiments [39–41] and theories [32, 39–42]. Therefore, the vacancy concentrations in these samples must be lower than the detection limit and the vacancy contribution was less than 1% as compared to the bulk.

Figure 1 shows the first lifetimes ($\tau_{1,\pm}$) obtained from the Cu + Cu, Cu + Fe, Cu + Co and Cu + Ni systems in magnetic field. The measurements were repeated by reversing magnetic field for 10 ~ 20 times, The average lifetimes were used for the further analysis. In the cases of the Cu + Fe and

Table 1. Experimental and theoretical (density functional theory (DFT))lifetimes (τ_{maj} and τ_{min}) associated with majority and minority spin electrons, field reversal of total annihilation rate (P_{λ}) determined from equation (8) and $P = 0.35$, of Fe, Co and Ni and the field reversal of three-gamma annihilation probabilities ($P^{3\gamma}$) in the previous work [6].

	Present	DFT [32]	Previous [6]
		Fe	
τ_{maj} (ps)	109 ± 2	95.2	
τ_{min} (ps)	120 ± 3	107.0	
P_{λ}	-0.018 ± 0.005	-0.021	$P^{3\gamma} : -0.0053 \pm 0.0009$
		Co	
τ_{maj} (ps)	100 ± 5	94.5	
τ_{min} (ps)	114 ± 5	98.2	
P_{λ}	-0.024 ± 0.012	-0.007	
		Ni	
τ_{maj} (ps)	106 ± 5	101.1	
τ_{min} (ps)	100 ± 5	96.8	
P_{λ}	0.010 ± 0.011	0.008	$P^{3\gamma} : 0.0012 \pm 0.0009$

Cu + Co, the lifetime shows no change upon field reversal. The lifetime also agrees with the bulk lifetime determined without magnetic field. In the other cases, the lifetimes change upon field reversal. In the cases of Cu + Fe and Cu + Co, the lifetimes in positive field are shorter than those in negative field, whereas, the relationship is opposite for the Cu + Ni. Table 1 lists the bulk lifetimes associated with the majority and minority spin electrons deduced from equations (4) and (7) and theoretical values by Lin *et al* [32].

Apart from the absolute differences between experiment and theory, the signs agree with each other. The results for the Fe and Co samples may be simply explained considering the fact that the number of majority spin electrons is more than that of minority spin electrons. According to Lin *et al* [32], the opposite tendency for the Ni sample can be explained as due to delocalized distribution of minority spin electrons in Ni. That is, the minority spins are broadened into interstitial regions and the minority spin densities there are larger than those of majority spins. According to the calculated MCP profiles for ferromagnetic nickel by Dixon *et al* [43], the first four bands are quite negative in the low momentum region, indicating that the delocalized states in real space are negatively polarized. Positron and electron wavefunctions have more overlapping in interstitial region. Hence, in the case of Ni, the lifetime associated with minority spin electrons may be shorter than that of majority spin electrons.

The field reversal of P_{λ} determined from the above positron lifetimes and $P = 0.35$ are also listed together with those by Lin *et al* [32] and $P^{3\gamma}$ by Berko and Mills (BM) [6] in table 1. Both the sign and magnitude of P_{λ} are in good agreement with those of the DFT calculation. However, two new works give significantly larger P_{λ} as compared to BM's $P^{3\gamma}$.

Figures 2(a)–(c) and 3(a)–(c) show the difference DBAR spectra of Fe single crystal obtained from measured DBAR spectra using equation (8) with the BM's $P^{3\gamma}$ [6] and P_{λ} by Lin *et al* [32], respectively, of which P is replaced with 0.6, along different momentum axes. The curves were smoothed by the five-point interpolation. The curve shapes in figures 2(a)–(c) are similar to what BM ever reported [6].

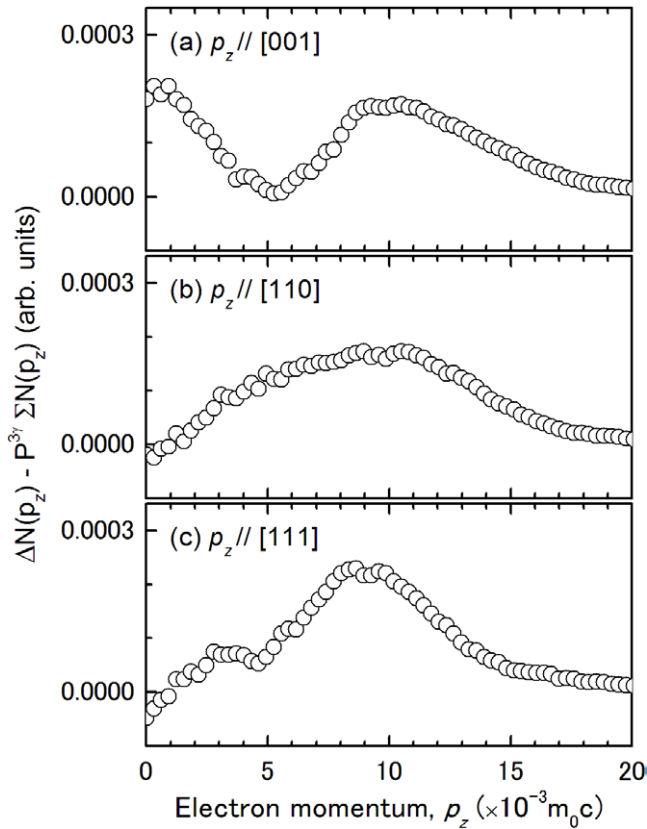


Figure 2. Experimental difference spectra between majority and minority spin bands of Fe using equation (8) and BM’s $P^{3\gamma}$ [6] instead of P_λ [32] in different momentum axes of (a) [0 0 1], (b) [1 1 0] and [1 1 1].

Contrarily, the curve shapes in figures 3(a)–(c) obtained using the present P_λ are rather different from the BM’s data [6]. Therefore, the problem is that, which of BM’s $P^{3\gamma}$ [6] or the present P_λ is more realistic. In figures 3(a)–(c), the calculated difference spectra between majority and minority spin bands are also shown. The experiment and the calculation are in good agreement when using the present P_λ . Probably the BM’s $P^{3\gamma}$ [6] was underestimated due to the extremely low counting rate. Nevertheless, in both figures 2 and 3, the curve shape depends on the momentum axis suggesting different momentum distributions along different directions.

In figures 3(a)–(c), along the [1 0 0] direction, a sharp peak and a shoulder appear in the lower momentum region and at around $p_z = 10 \times 10^{-3} m_0 c$, respectively. Along the [1 1 0] and [1 1 1] directions, the shapes are more gentle. In figure 3(a), no clear evidence about negative spin polarization of s electrons is seen since the spectrum shows no dip at around $p_z = 0$. In figures 3(b) and (c), although no dips appear at around $p_z = 0$, the intensities are reduced as compared to figure 3(a). This may be explained by negative spin polarization of s electrons. From the comparison with the calculated curves, the bands 3 and 4 give rise to such features. The bands 1 and 2 have more s -like character, but their contributions to the spectra are very small probably due to the small density of state and more positive spin polarization. The bands 5 and 6 have more d -like dispersion along any directions making over all broad spectrum shapes.

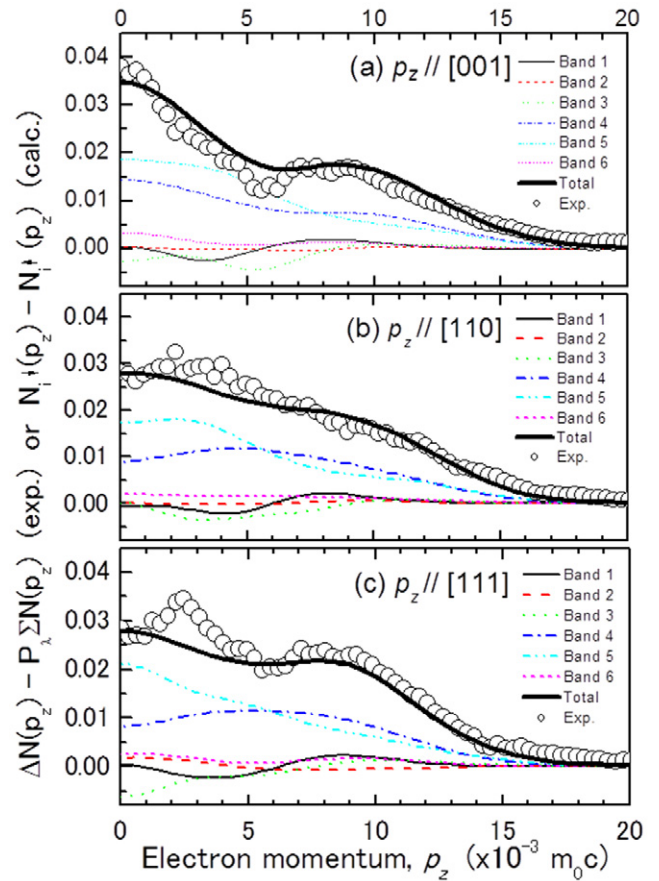


Figure 3. Experimental and calculated difference spectra between majority and minority spin bands of Fe using equation (8) and P_λ [32] and theoretical curves in different momentum axes of (a) [0 0 1], (b) [1 1 0] and [1 1 1].

5. Conclusion

In conclusion, we measured spin-dependent positron lifetimes for Fe, Co and Ni. The differences of bulk positron lifetimes associated with majority and minority spin electrons were confirmed. The yielded difference DBAR spectra between majority and minority spin electrons using the two spin-dependent Fe bulk lifetimes were well consistent with the theoretical calculations. This study shows that spin-polarized positron lifetime technique can be used in analysis of spin-aligned electron momentum distribution.

Acknowledgments

We thank M Saito and J B Lin of Kanazawa University for their valuable comments about theoretical calculations. This work was supported by JSPS KAKENHI Grant No.24310072.

References

- [1] Hanna S S and Preston R S 1957 *Phys. Rev.* **106** 1363–4
- [2] Wu C S, Ambler E, Hayward R W, Hoppes D D and Hudson R P 1957 *Phys. Rev.* **105** 1413–5
- [3] Hanna S S and Preston R S 1958 *Phys. Rev.* **109** 716–20
- [4] Berko S and Zuckerman J 1964 *Phys. Rev. Lett.* **13** 339–41

- [5] Berko S 1967 *Positron Annihilation* (New York: Academic) p 61
- [6] Berko S and Mills A 1971 *J. Phys. Colloq.* **32** C1–287
- [7] Mijnders P and Hambro L 1964 *Phys. Lett.* **10** 272–3
- [8] Mihalisin T and Parks R 1966 *Phys. Lett.* **21** 610–1
- [9] Mihalisin T W and Parks R D 1967 *Phys. Rev. Lett.* **18** 210–1
- [10] Mihalisin T and Parks R 1969 *Solid State Commun.* **7** 33–5
- [11] Mijnders P 1973 *Physica* **63** 248–62
- [12] Shiotani N, Okada T, Sekizawa H, Mizoguchi T and Karasawa T 1973 *J. Phys. Soc. Japan* **35** 456–60
- [13] Hohenemser C, Weingart J and Berko S 1968 *Phys. Lett. A* **28** 41–2
- [14] Šob M, Szuszkiewicz S and Szuszkiewicz M 1984 *Phys. Status Solidi b* **123** 649–52
- [15] Jarlborg T, Manuel A, Mathys Y, Peter M, Singh A and Walker E 1986 *J. Magn. Magn. Mater.* **54–7** 1023–4
- [16] Szuszkiewicz S, Šob M and Szuszkiewicz M 1986 *J. Magn. Magn. Mater.* **62** 202–4
- [17] Genoud P, Singh A K, Manuel A A, Jarlborg T, Walker E, Peter M and Weller M 1988 *J. Phys. F* **18** 1933
- [18] Genoud P, Manuel A A, Walker E and Peter M 1991 *J. Phys.: Condens. Matter* **3** 4201
- [19] Kondo H, Kubota T, Nakashima H, Kawano T and Tanigawa S 1992 *J. Phys.: Condens. Matter* **4** 4595
- [20] Hanssen K, Mijnders P, Rabou L and Buschow K 1990 *Phys. Rev. B* **42** 1533
- [21] Hanssen K and Mijnders P 1986 *Phys. Rev. B* **34** 5009
- [22] Haynes T, Watts R, Laverock J, Major Z, Alam M, Taylor J, Duffy J and Dugdale S 2012 *New J. Phys.* **14** 035020
- [23] Dugdale S 2014 *Low Temp. Phys.* **40** 328–38
- [24] Kawasuso A, Maekawa M, Fukaya Y, Yabuuchi A and Mochizuki I 2011 *Phys. Rev. B* **83** 100406
- [25] Kawasuso A, Maekawa M, Fukaya Y, Yabuuchi A and Mochizuki I 2012 *Phys. Rev. B* **85** 024417
- [26] Maekawa M, Fukaya Y, Yabuuchi A, Mochizuki I and Kawasuso A 2013 *Nucl. Instrum. Meth. B* **308** 9–14
- [27] Maekawa M, Fukaya Y, Zhang H, Li H and Kawasuso A 2014 *J. Phys. Conf. Ser.* **505** 012033
- [28] Cooper M J 1985 *Rep. Prog. Phys.* **48** 415
- [29] Cooper M and Bansil A 2004 *X-Ray Compton Scattering* (New York: Oxford University Press)
- [30] Gidley D W, Köymen A R and Capehart T W 1982 *Phys. Rev. Lett.* **49** 1779–83
- [31] Deckers C, Greif H, Knichel W, Maier K, Tongbhoyai M, Siegle A, Ehmann J and Schneider H 1995 *Phys. Lett. A* **197** 179–82
- [32] Lin J, Yamasaki T and Saito M 2014 *Japan. J. Appl. Phys.* **53** 053002
- [33] Dirac P A 1930 *Mathematical Proc. of the Cambridge Philosophical Society* vol 26 (Cambridge: Cambridge University Press) pp 376–85
- [34] Boroński E and Nieminen R M 1986 *Phys. Rev. B* **34** 3820–31
- [35] Gonze X *et al* 2002 *Comput. Mater. Sci.* **25** 478
- [36] Bloöchl P E 1994 *Phys. Rev. B* **50** 17953
- [37] Maekawa M, Fukaya Y, Yabuuchi Y and Kawasuso A 2011 *J. Phys. Conf. Ser.* **262** 012035
- [38] Kirkegaard P and Eldrup M 1974 *Comput. Phys. Commun.* **7** 401–9
- [39] Ohkubo H, Tang Z, Nagai Y, Hasegawa M, Tawara T and Kiritani M 2003 *Mater. Sci. Eng. B* **350** 95–101
- [40] Robles J M C, Ogando E and Plazaola F 2007 *J. Phys.: Condens. Matter* **19** 176222
- [41] Welch D O and Lynn K G 1976 *Phys. Status Solidi b* **77** 277–86
- [42] Puska M J and Nieminen R M 1994 *Rev. Mod. Phys.* **66** 841–97
- [43] Dixon M, Duffy J, Gardelis S, McCarthy J, Cooper M, Dugdale S, Jarlborg T and Timms D 1998 *J. Phys.: Condens. Matter* **10** 2759